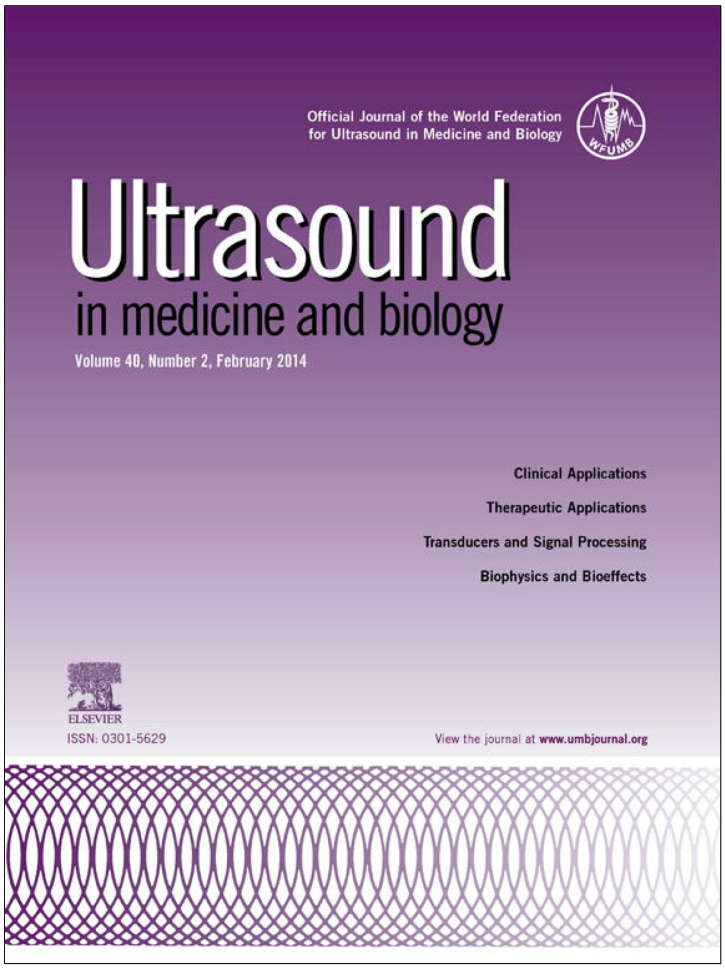

Ultrasound in Med. & Biol., Vol. 40, No. 2, pp. 410–421, 2014

0301-5629/$ - see front matter

http://dx.doi.org/10.1016/j.ultrasmedbio.2013.09.018

● *Original Contribution*

# BROADBAND ATTENUATION MEASUREMENTS OF PHOSPHOLIPID-SHELLED ULTRASOUND CONTRAST AGENTS

JASON L. RAYMOND,* KEVIN J. HAWORTH,*† KENNETH B. BADER,† KIRTHI RADHAKRISHNAN,* JOSEPH K. GRIFFIN,* SHAO-LING HUANG,‡ DAVID D. MCPHERSON,‡ and CHRISTY K. HOLLAND*†

*Biomedical Engineering Program, University of Cincinnati, Cincinnati, Ohio, USA; †Division of Cardiovascular Diseases, Department of Internal Medicine, University of Cincinnati, Cincinnati, Ohio, USA; and ‡Division of Cardiology, Department of Internal Medicine, University of Texas Health Science Center at Houston, Houston, Texas, USA

(*Received* 17 *June* 2013; *revised* 3 *September* 2013; *in final form* 13 *September* 2013)

**Abstract—The aim of this study was to characterize the frequency-dependent acoustic attenuation of three phospholipid-shelled ultrasound contrast agents (UCAs): Definity, MicroMarker and echogenic liposomes. A broadband through-transmission technique allowed for measurement over 2 to 25 MHz with a single pair of transducers. Viscoelastic shell parameters of the UCAs were estimated using a linearized model developed by N. de Jong, L. Hoff, T. Skotland and N. Bom (Ultrasonics 1992; 30:95–103). The effect of diluent on the attenuation of these UCA suspensions was evaluated by performing attenuation measurements in 0.5% (w/v) bovine serum albumin and whole blood. Changes in attenuation and shell parameters of the UCAs were investigated at room temperature (25°C) and physiologic temperature (37°C). The attenuation of the UCAs diluted in 0.5% (w/v) bovine serum albumin was found to be identical to the attenuation of UCAs in whole blood. For each UCA, attenuation was higher at 37°C than at 25°C, underscoring the importance of conducting characterization studies at physiologic temperature. Echogenic liposomes exhibited a larger increase in attenuation at 37°C versus 25°C than either Definity or MicroMarker. (E-mail: raymonjl@mail.uc.edu)** **© 2014 World Federation for Ultrasound in Medicine & Biology.**

***Key Words:*** **Ultrasound contrast agents, Microbubbles, Broadband characterization, Size distribution, Polyvinylidene fluoride transducer, Echogenic liposomes, Definity, MicroMarker.**

## INTRODUCTION

The use of microbubbles as ultrasound contrast agents (UCAs) in vascular imaging is well established. Contrast-enhanced ultrasound imaging of arteries has been used as a non-invasive method for screening patients at risk for cardiovascular events, identifying disease progression and monitoring the effectiveness of preventive therapies (Feinstein 2006). Techniques that use UCAs in therapeutic applications, such as drug and gene delivery (Bekeredjian et al. 2005; Laing and McPherson 2009; Sutton et al. 2013), are also under active development. Phospholipid-based UCAs are of particular interest because they can be targeted to molecular components of atherosclerotic disease by attaching specific ligands to their surfaces (Elbayoumi and Torchilin 2008; Klegerman et al. 2010; Klibanov 2006; Kornmann et al. 2010; Lindner 2004; Weissig 2010).

One such UCA under development is echogenic liposomes (ELIP) (Alkan-Onyuksel et al. 1996; Demos et al. 1999; Hitchcock et al. 2010; Huang et al. 2001; Paul et al. 2012). These agents consist of phospholipid vesicles enclosing both an aqueous space and entrapped gas. ELIP are echogenic because of the presence of air, which is entrapped and stabilized by the lipid during the rehydration process (Huang 2010). Previous studies have suggested that the freeze-drying procedure is key to the generation of defects in the lipid bilayers that, on rehydration, fuse and trap small amounts of air (Huang et al. 2001, 2002). ELIP formulations differ from other commercially available contrast agents primarily in size, shell material and gas content. Most commercially available contrast agents have mean diameters between 1 and 5 $\mu$m and consist of microbubbles encapsulated by a protein, polymer or lipid shell (Stride 2009). These agents typically contain high-molecular-weight gases, which have low solubility in blood and, thus, increase the lifetime of the microbubbles in circulation (Qin et al. 2009; Sarkar et al. 2009). ELIP have a phospholipid bilayer shell and include a small amount

Address correspondence to: Jason L. Raymond, Cardiovascular Center, CVC 3940, University of Cincinnati, Cincinnati, OH 45267-0586, USA. E-mail: raymonjl@mail.uc.edu

of cholesterol, which acts to increase membrane rigidity (Huang et al. 2001). ELIP range in size from ~70 nm to several microns (Kopechek et al. 2011; Paul et al. 2012). ELIP formulations contain air, which is more soluble in blood than high-molecular-weight gases. However, ELIP with optimized lipid formulations have been shown to be echogenic and stable under physiologic conditions for tens of minutes (Buchanan et al. 2008; Radhakrishnan et al. 2012). The exact location of the entrapped air pockets in ELIP has not been fully ascertained, possibly because air pockets are stabilized by lipid monolayers within the liposome or by the lipid bilayer shell (Huang 2008).

Previous acoustic characterization studies by Kopechek et al. (2011) and Paul et al. (2012) revealed that the scattering properties of ELIP are suitable for various ultrasound imaging applications including intravascular ultrasound (20 MHz or higher), as well as fundamental and harmonic imaging (3–12 MHz). In both of these studies, several transducers were used to cover the frequency range for attenuation measurements. Furthermore, both studies were conducted at room temperature. Recent work by Mulvana et al. (2010) indicates that the acoustic characteristics of the phospholipid-based UCA SonoVue are affected by temperature in the range 20°C–40°C for transvascular diagnostic frequencies (1–6 MHz). Vos et al. (2008) also investigated the influence of temperature (22°C vs. 37°C) on ultrasound excitation of SonoVue and Definity using optical techniques. However, the effect of temperature on the acoustic characteristics of phospholipid-based UCAs over both transvascular and intravascular frequencies has not been fully determined.

The objective of the present study was to investigate the shell properties of phospholipid-based UCAs over a broad frequency range at room temperature and also under physiologic conditions. We hypothesize that the temperature dependence noted by Mulvana et al. (2010) will be evident in other phospholipid-based UCAs and may also depend on frequency. These differences may affect the optimal insonation parameters for diagnostic as well as therapeutic applications (Laing and McPherson 2009; Qin et al. 2009). Lipid shells have a wide variety of material properties. Therefore, three formulations of ELIP, as well as two commercially available phospholipid-based UCAs, Definity and MicroMarker, were characterized in this study. Definity is a commercially available UCA that has been approved by the U.S. Food and Drug Administration for left ventricular opacification in patients with sub-optimal echocardiograms (Patil and Main 2012). MicroMarker is a contrast agent developed specifically for pre-clinical high-frequency (>20 MHz) ultrasound imaging (Bracco Research, Geneva, Switzerland). According to the manufacturer, this agent was developed on the same principles as the second-generation clinical contrast agent SonoVue (VisualSonics Rev 1.4). We compared the measured attenuation of the UCAs at 25°C and 37°C. The following sections provide background on the methodology used to assess shell parameters. Finally, the results of attenuation measurements and estimated values for shell parameters are discussed.

## METHODS

### *Agent handling and preparation*

*Definity.* Definity (perflutren lipid microspheres; Lantheus Medical Imaging, North Billerica, MA, USA) consists of octofluoropropane ($C_3F_8$) microbubbles encapsulated by a lipid shell monolayer composed of three phospholipids. Vials of Definity were activated according to the manufacturer's instructions. Briefly, a vial was removed from refrigeration and allowed to warm to room temperature (20°C–24°C) before activation by shaking for 45 s using a Vial-Mix (Lantheus Medical Imaging). All measurements were performed within 1 h of activation, and the agent was resuspended by hand agitation (inverting the vial) for 10 s before each withdrawal. A 20-gauge needle was used to withdraw the agent from the middle of the vial.

*MicroMarker.* Vevo MicroMarker (VisualSonics, Toronto, ON, Canada; Bracco Research, Geneva, Switzerland) consists of a mixture of nitrogen and perfluorobutane gas ($C_4F_{10}$) encapsulated by a monolayer shell composed of polyethylene glycol, phospholipids and fatty acids (VisualSonics PN11691). The agent was prepared according to the manufacturer's directions by injecting 0.7 mL of saline (0.9% w/v) into the vial using a 21-gauge needle. The syringe was detached from the needle, which was left in the vial to vent to atmospheric pressure for a few seconds and then removed. The vial was agitated by hand for 1 min and allowed to rest for 10 min at room temperature before the sample was withdrawn using a 20-gauge needle.

*Echogenic liposomes.* Three formulations of ELIP, each previously described (Buchanan et al. 2008; Huang et al. 2002; Tiukinhoy-Laing et al. 2007), were evaluated in this study. The original formulation described by Huang et al. (2002) consists of L-$\alpha$-phosphatidylcholine (EggPC), 1,2-dipalmitoyl-*sn*-glycero-3-phosphoethanolamine (DPPE), 1,2-dipalmitoyl-*sn*-glycero-3-phospho-[1′-rac-glycerol] (DPPG) and cholesterol (CH) in a molar ratio of 69:8:8:15. This formulation, which is referred to as ELIP, resulted in an echogenic dispersion after preparation using a process involving sonication of the lipid in water,

addition of mannitol, freezing, lyophilization and rehydration (Huang et al. 2002).

The duration of echogenicity of the original ELIP formulation was improved by replacing approximately one-third of the unsaturated EggPC with saturated 1,2-dipalmitoyl-*sn*-glycero-3-phosphocholine (DPPC). This formulation (EggPC/DPPC/DPPE/DPPG/CH molar ratio of 27:42:8:8:15), which is called enhanced ELIP in this article, resulted in retention of echogenicity after 1 h at physiologic temperature (Buchanan et al. 2008).

To assess the effect of drug loading on the shell properties of ELIP, a third formulation was considered that involved incorporation of the thrombolytic drug recombinant tissue plasminogen activator (rt-PA). ELIP loaded with rt-PA were developed to aid visualization of the site of arterial occlusion and release the thrombolytic drug locally (Smith et al. 2010; Tiukinhoy-Laing et al. 2007). Smith et al. (2010) found that ELIP loaded with rt-PA are echogenic during continuous fundamental B-mode imaging and can be rapidly fragmented with color Doppler pulsed ultrasound. The lipid composition used for rt-PA-loaded ELIP included 1,2-dioleoyl-*sn*-glycero-3-phosphocholine (DOPC) and had a DPPC/DOPC/DPPG/CH molar ratio of 46:24:24:6 (Tiukinhoy-Laing et al. 2007).

Each of the ELIP formulations was prepared using the method developed by Huang and MacDonald (2004), which involves freezing in the presence of mannitol, followed by lyophilization and rehydration of the lipid suspension (Huang 2010). All lipids were purchased from Avanti Polar Lipids (Alabaster, AL, USA). Stock suspensions of ELIP were prepared by reconstituting 6 mg lyophilized lipid powder using 0.6 mL air-saturated, filtered (0.2-$\mu$m) and deionized water (NANOPure, Barnstead International, Dubuque, IA, USA) at room temperature (20°C–24°C), yielding a stock solution with a lipid concentration of 10 mg/mL.

*Particle size measurement*

The size distribution of each UCA was measured using a Coulter counter (Multisizer 4, Beckman Coulter, Brea, CA, USA) with a 30-$\mu$m aperture tube and 100-$\mu$L volumetric setting. Agents were diluted in air-saturated phosphate-buffered saline (PBS, 0.9% w/v; Sigma Chemical, St. Louis, MO, USA) to an approximate concentration of $10^5$ particles/100 $\mu$L sample volume to avoid blockage of the aperture and to reduce coincident particle flow through the aperture. The number density of particles (corrected for dilution) was returned as a histogram consisting of 200 bins logarithmically spaced from 0.6 to 18 $\mu$m. The measurement was repeated five times for each sample, and the mean and standard deviation of the number density of particles were computed. The volume-weighted concentration was calculated from the number of bubbles per unit volume within each bin.

*Broadband attenuation measurement*

A diagram of the experimental setup for acoustic attenuation measurements is provided in Figure 1. Measurements were conducted in a 22-L acrylic tank (17 × 9 × 9 in.) filled with distilled water maintained at either 25 ± 0.5°C or 37 ± 0.5°C using a circulating water bath (Neslab EX, Newington, NH, USA). A pair of broadband polyvinylidene fluoride (PVDF) transducers (6.35-mm diameter, 38.1-mm focal length, 20-MHz center frequency; PI-20, Olympus NDT, Waltham, MA, USA) were used to acquire the through-transmission spectrum using a broadband pulse technique (Marsh et al. 1997). An ultrasound pulser-receiver (Panametrics 5077 PR, Olympus NDT) was used to generate the excitation pulse (pulse repetition frequency = 100 Hz) and amplify the received signal (20- to 50-dB gain). The transmit pulse amplitude was controlled using an in-line variable attenuator (SA-50, Texscan, Indianapolis, IN, USA). Absolute acoustic pressure output was calibrated using a 0.4-$\mu$m membrane hydrophone (Precision Acoustics, Dorchester, Dorset, UK). Peak positive and negative pressures were 24 and 31 kPa (±12% uncertainty), respectively, at the location of the front face of the sample chamber, which was 60 mm from transmit transducer. The asymmetric peak positive and peak negative pressures were a result of the short pulse and frequency response of the transducer. The spectral content of the transmitted pulses did not change because of non-linearities for acoustic pressures

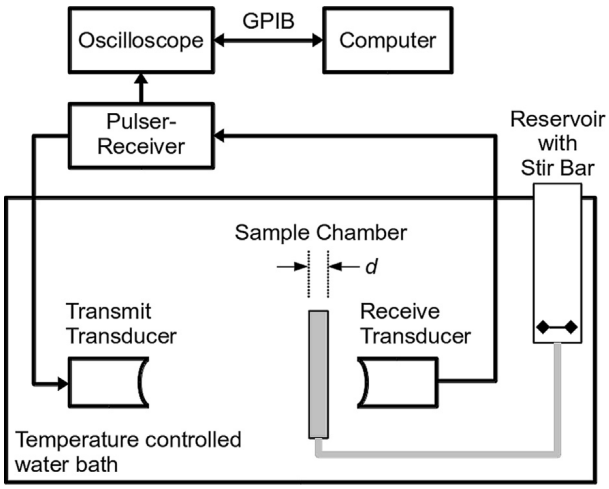


Fig. 1. Schematic of the attenuation measurement setup. A pair of broadband polyvinylidene fluoride transducers were employed to acquire the spectrum using a substitution technique. A pulser-receiver was used in through-transmission mode to generate the excitation pulse and amplify the received signal. Samples of ultrasound contrast agents in diluent or diluent alone were added to the reservoir and introduced into the sample chamber by gravity feed. GPIB = general purpose interface bus.

less than 150 kPa. Received waveforms were averaged (256 traces per acquisition), digitized (LT572, LeCroy, Chestnut Ridge, NY, USA; 16 bits, 1-GHz sampling rate) and transferred to a computer for analysis using MATLAB (The MathWorks, Natick, MA, USA). The sample chamber consisted of an unmodified cell culture cassette (CLINIcell 25, Mabio, Tourcoing, France) with acoustically transparent polycarbonate film windows (25-cm$^2$ area, 175-$\mu$m thick) and a rigid polycarbonate frame with luer-lock ports for introducing the sample suspension. A reservoir was used for mixing the diluent and UCAs before introduction of the suspension into the sample chamber by gravity feed. Samples of diluent alone or diluent with UCAs were added to the reservoir and mixed using a magnetic stirrer before the attenuation measurement.

The frequency-dependent attenuation coefficient, $\alpha(f)$ (in dB/cm), was determined using a broadband substitution technique (American Institute of Ultrasound in Medicine [AIUM] 1995). The attenuation spectrum is computed from the measured voltage-time waveforms

$$\alpha_{\text{meas}}(f) = 10\log_{10}\left(\frac{\left|V_{\text{ref}}(f)\right|^2}{\left|V_{\text{sample}}(f)\right|^2}\right)\Big/ d \qquad (1)$$

where $V_{\text{ref}}$ and $V_{\text{sample}}$ are the received amplitude spectra in the absence (diluent alone) and presence of the UCA, respectively, and $d$ is the path length over which the acoustic wave interacts with the sample suspension (4.6 mm). Attenuation was measured over the frequency range 2 to 25 MHz, corresponding to the –20-dB bandwidth of the system.

*Determination of effect of diluent and temperature on attenuation measurements*

Attenuation measurements were performed by diluting the UCA sample in either human whole blood or a solution of PBS and 0.5% (w/v) albumin. Each of the diluents was saturated with air at room temperature before conducting the attenuation measurements at either room temperature (25 ± 0.5°C) or physiologic temperature (37 ± 0.5°C).

Approval from the local institutional review board was obtained for use of human blood samples from incomplete phlebotomy procedures (Hoxworth Blood Center, Cincinnati, OH, USA). Approximately 100 mL of whole blood containing citrate phosphate double dextrose (CP2-D) anticoagulant was titrated to pH 7.4 and allowed to equilibrate at room temperature while being stirred gently for at least 2 h. A blood gas meter (i-STAT CG4+, Abbot Point of Care, Princeton, NJ, USA) was used to measure the partial pressures of oxygen ($pO_2$) and carbon dioxide ($pCO_2$). Based on the handling of the whole blood *in vitro*, the total partial pressure of oxygen and carbon dioxide was considered to be proportional to the total dissolved gas and was measured to be 136 ± 5 mm Hg. The total partial pressure of oxygen and carbon dioxide in human arterial blood is ~134 mm Hg, whereas the total partial pressure of all dissolved gases is slightly less than 1 atm (Altman 1958).

Phosphate-buffered saline at room temperature was gently bubbled with air while stirring for approximately 20 min before lyophilized albumin powder (Sigma Chemical Co.) was added to yield a 0.5% (w/v) solution. A dissolved oxygen meter (DO 110; Oakton Instruments, Vernon Hills, IL, USA) was used to measure the oxygen saturation (100 ± 1%) before attenuation measurements.

*Estimation of shell parameters*

Shell properties were determined using a linearized acoustic model proposed by de Jong et al. (1992; de Jong and Hoff 1993) in which the UCA shell is characterized by *ad hoc* parameters for shell elasticity ($S_p$ in N/m) and shell friction ($S_f$ in kg/s) (de Jong and Hoff 1993). This method has been used extensively to model the acoustic response of UCAs and to quantify UCA shell parameters. Details of the model are available in the literature (Faez et al. 2011; Goertz et al. 2007; Gorce et al. 2000). This theory does not account for bubble-bubble interactions and ignores multiple scattering, which is commonly assumed for dilute suspensions used for UCA characterization (Chen and Zhu 2006; Marsh et al. 1997; Stride and Saffari 2005). In this regime, the power lost by the ultrasound wave is the sum of the power absorbed by the individual microbubbles in the suspension. The acoustic attenuation per unit distance is given by

$$\alpha_{\text{est}}(f, S_p, S_f) = 10(\log_{10} e) N_{\text{fit}} \sum_k \sigma_e(r_k, f, S_p, S_f) n_k \qquad (2)$$

where $N_{\text{fit}}$ is the total number of bubbles per unit volume, and $n_k$ is the normalized number distribution of bubbles with radius $r_k$. Each microbubble contributes to the attenuation of a particular frequency component ($f$) according to its extinction cross section, $\sigma_e$, which is defined in de Jong et al. (1992) as

$$\sigma_e(r, f, S_p, S_f) = \frac{4\pi r^2}{\left[\left(f_0^2(r, S_p)/f^2\right) - 1\right]^2 + \delta_{\text{tot}}^2(r, f, S_f)} \cdot \frac{\delta_{\text{tot}}^2(r, f, S_f)}{\delta_{\text{rad}}^2(r, f)} \qquad (3)$$

where $f_0$ is the resonance frequency for a shelled microbubble with radius $r$, $\delta_{tot}$ is the total damping coefficient and $\delta_{rad}$ is the damping caused by acoustic radiation.

Estimates of shell parameters and number density of microbubbles were obtained by partitioning the general ordinary-least-squares (OLS) model (Whittle 1983). Because echogenic liposome suspensions contain particles with aqueous cores in addition to microbubbles, it was necessary to differentiate between the number density of *particles* measured directly by the Coulter counter and the number density of *microbubbles,* which contribute to the attenuation spectra. Liposomes that contain only aqueous cores do not contribute to the measured attenuation spectrum and, therefore, were not included in the acoustic model. The number density of microbubbles contributing to attenuation ($N_{fit}$) was empirically determined by minimizing the sum of the deviations of the predicted values from the mean of the measured response. The size distribution of bubbles is assumed to be proportional to the number of particles as measured with the Coulter counter. Estimates of shell parameters are obtained by minimizing the sum-squared difference of errors between the estimated and measured attenuation coefficients, with a corresponding error function defined by

$$\mathrm{Err}\left(N_{fit}, S_p, S_f\right) = \sum_i \left(\alpha_{est}\left(f_i, N_{fit}, S_p, S_f\right) - \alpha_{meas}\left(f_i\right)\right)^2 \quad (4)$$

where $\alpha_{est}$ are the estimated attenuation coefficients, and $\alpha_{meas}$ are the measured attenuation coefficients (Faez et al. 2011). The values of the shell parameters that corresponded to a doubling of the error function value were taken to be the limits for the confidence interval (Hoff et al. 2001). The coefficient of determination ($R^2$) was calculated to indicate how well the estimated attenuation coefficients fit the measured data.

Values of the physical parameters used for the diluent (PBS with 0.5% (w/v) albumin solution) were measured in the laboratory and are given in Table 1. Sound speed was determined by measuring the difference in arrival time between multiple successive echoes using a 1-cm quartz cuvette. Liquid viscosity was measured using a glass capillary viscometer (modified Ostwald type, size 100; Industrial Research Glassware, Kenilworth, NJ, USA). For each measurement, samples were maintained at either 25 ± 0.5°C or 37 ± 0.5°C using a circulating water bath (Neslab EX). Table 2 summarizes the UCAs and dilution ratios used for broadband attenuation measurements. The ratio of specific heats for the gases was taken to be 1.4, 1.09 and 1.07 for air, $C_3F_8$ and $C_4F_{10}$, respectively.

Table 1. Physical constants for phosphate-buffered saline with 0.5% (w/v) albumin solution

| | | Value | |
|---|---|---|---|
| Constant | Units | 25°C | 37°C |
| Sound speed | $m\ s^{-1}$ | 1505 | 1536 |
| Density | $kg\ m^{-3}$ | 1011 | 1007 |
| Dynamic viscosity | $kg\ (m\ s)^{-1}$ | $0.93 \times 10^{-3}$ | $0.76 \times 10^{-3}$ |

## RESULTS

### *Size distribution measurements*

The measured size distribution for each contrast agent is illustrated in Figure 2. Both number-weighted distributions (gray histogram) and volume-weighted distributions (black line) are provided. The volume-weighted size distributions for Definity (1.6 μm), MicroMarker (2.3 μm), ELIP (1.3-1.5 μm), enhanced ELIP (2.1 μm) and rt-PA-loaded ELIP (2.0 μm) each peaked between 1 and 3 μm. Definity exhibited a bimodal distribution with a second peak at ~6 μm, consistent with other measurements for Definity reported in the literature (Faez et al. 2011; Goertz et al. 2007; Helfield et al. 2012; Stapleton et al. 2009).

### *Effect of diluent on attenuation measurements*

Figure 3 compares measured attenuation spectra averaged over three trials (N = 3) for enhanced ELIP in human whole blood and PBS with 0.5% albumin at 37°C. There was very good agreement between attenuation of ELIP in whole blood and attenuation of ELIP in the PBS + 0.5% albumin solution. Therefore, PBS with 0.5% albumin was used as a surrogate diluent for the attenuation measurements.

### *Effect of temperature on attenuation measurements*

Figure 4 illustrates the measured attenuation coefficients as a function of frequency at 25°C and 37°C for Definity, MicroMarker, ELIP, enhanced ELIP and

Table 2. Contrast agents and dilution ratios used for attenuation measurements

| Agent | Gas | Dilution ratio |
|---|---|---|
| Definity | $C_3F_8$ | 1:2000 |
| MicroMarker | $C_4F_{10}$ | 1:500 |
| ELIP | Air | 1:200 |
| Enhanced ELIP | Air | 1:200 |
| rt-PA-loaded ELIP | Air | 1:200 |

ELIP = echogenic liposomes; rt-PA = recombinant tissue plasminogen activator.

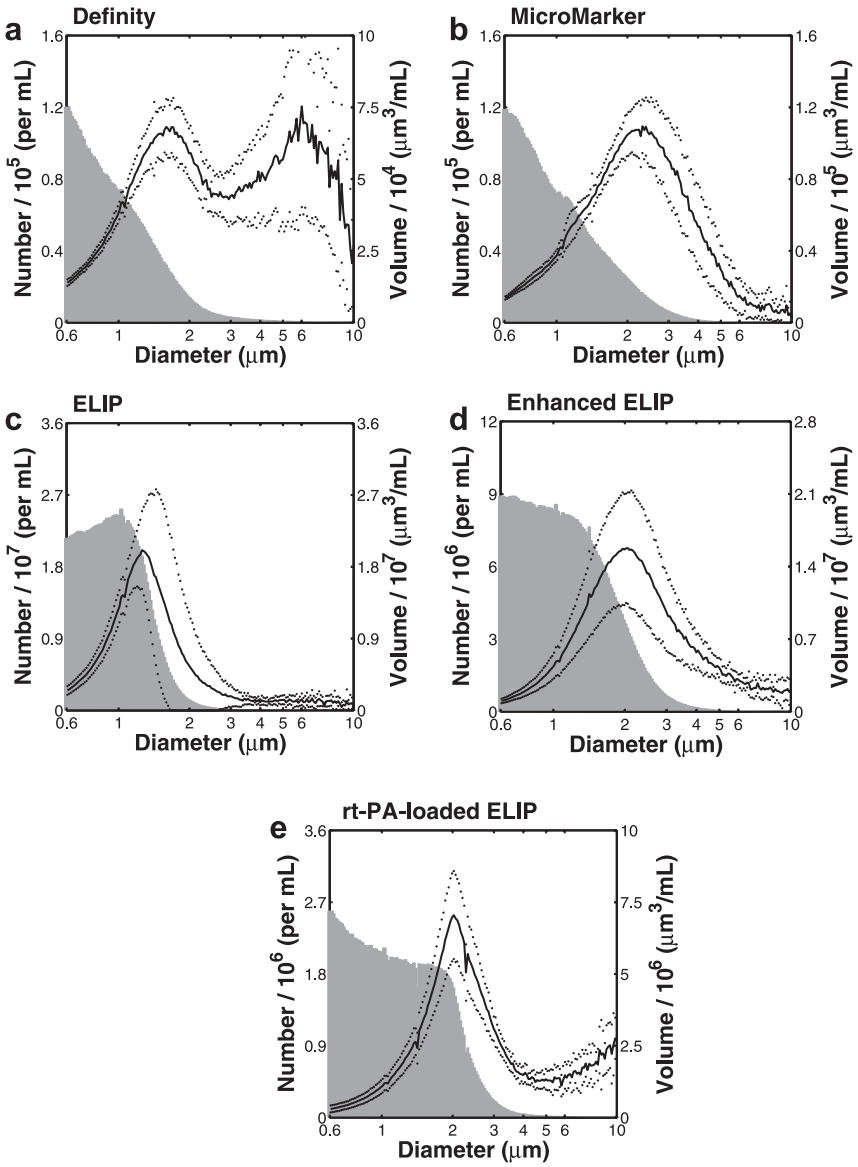


Fig. 2. Coulter counter size distribution measurements for (a) Definity, (b) MicroMarker, (c) echogenic liposomes (ELIP), (d) enhanced ELIP and (e) recombinant tissue plasminogen activator (rt-PA)-loaded ELIP. Mean number density (histogram, *shaded*) and volume-weighted size distribution (*solid line*) are plotted versus particle diameter (note logarithmic scale on the abscissa). The dotted lines represent one standard deviation of the volume-weighted size distribution. Dilution ratios are given in Table 2. Data are truncated at a diameter of 10 $\mu$m for clarity.

rt-PA-loaded ELIP. The attenuation spectra were found to depend on diluent temperature (25°C or 37°C). All of the UCAs exhibited an increase in attenuation across most frequencies when measured at physiologic temperature compared with room temperature. For Definity (Fig. 4a), there was a slight decrease in the frequency of peak attenuation, whereas for MicroMarker and the three ELIP formulations (Figs. 4b–e), there was a slight increase in the frequency of peak attenuation at 37°C compared with room temperature. The experimentally measured attenuation coefficients of Definity and MicroMarker at 25°C or 37°C did not differ by more than one standard deviation in the frequency range ~2–7 MHz (Fig. 4a,b). Definity exhibited a 4.6-dB increase in the peak attenuation, whereas peak attenuation increased by 4.4, 8.8 and 6.4 dB for ELIP, enhanced ELIP and rt-PA-loaded ELIP, respectively. The peak attenuation of MicroMarkerdid not differ by more than one standard deviation at 37°C versus 25°C.

*Estimates of shell parameters*

Figure 5 illustrates the measured attenuation coefficients as a function of frequency, as well as the theoretical fits based on the estimated shell parameters, for Definity,

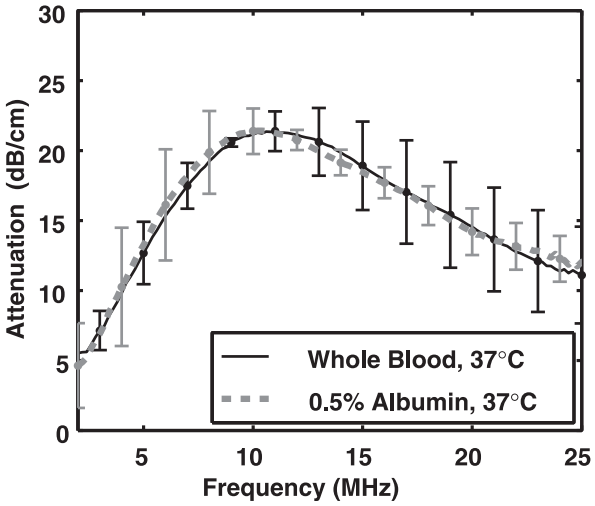


Fig. 3. Measured attenuation spectra for enhanced echogenic liposomes in whole blood (*solid line, black*) and phosphate-buffered saline with 0.5% (w/v) albumin (*dashed line, gray*).

MicroMarker, ELIP, enhanced ELIP and rt-PA-loaded ELIP at 37°C. The theoretical fits of the attenuation coefficients are in good agreement with the experimentally measured attenuation coefficients ($R^2 > 0.9$). Shell parameters determined by the best fit to the measured data are summarized in Table 3. The shell elasticity parameter ($S_p$) for the three ELIP formulations was higher at 3°C than at 25°C. It should be noted that a relatively small proportion of ELIP was found to contribute to the attenuation spectra at either 25°C or 37°C (Table 3). However, the number of particles that contributed to the attenuation (and, therefore, are assumed to contain microbubbles) was two to three times higher at 37°C than at 25°C for all ELIP formulations.

## DISCUSSION

Characterization of UCAs using acoustic attenuation measurements obtained with methods similar to those described here are well established (Chatterjee et al. 2005; de Jong and Hoff, 1993; de Jong et al. 1992; Hoff et al. 2000; Marsh et al. 1997; Sarkar et al. 2005). The shell properties of phospholipid-based agents such as SonoVue (Gorce et al. 2000), Definity (Faez et al. 2011; Goertz et al. 2007) and echogenic liposomes (Kopechek et al. 2011) have been characterized using acoustic attenuation measurements conducted at room temperature. The attenuation results at 25°C that are reported here are in agreement with these previously published values. Other recent *in vitro* studies have focused on the effect of temperature on the acoustic response of contrast agents. Using optical techniques, Vos et al. (2008) observed lower thresholds of acoustic activation and higher radial expansions of SonoVue and Definity at body temperature (37°C) compared with room temperature. Mulvana et al. (2010) observed a concomitant increase in acoustic attenuation and scattering for SonoVue at higher temperatures. The present study establishes a qualitatively similar result for the attenuation of Definity, MicroMarker and ELIP.

Definity exhibited an increase in attenuation across most frequencies when measured at 37°C versus 22°C (Fig. 4a). The frequency of peak attenuation for Definity also shifted to a lower value at 37°C. Because the resonance frequency of a bubble decreases with increasing diameter, this change suggests that the mean diameter of the microbubble population may be slightly larger at 37°C than at 25°C. The change in particle size distribution was not assessed in this study because the Coulter counter measurements were conducted only at room temperature (25°C). Mulvana et al. (2010) optically observed a change in mean diameter for SonoVue. They found a reduction in the relative number of bubbles with a diameter less than 2 $\mu$m and an increase in the mean bubble diameter at higher temperatures. Mulvana et al. hypothesized that gas expansion of the bubbles or gas diffusion into the bubbles resulted in an increase in bubble diameter with increasing temperature. Furthermore, they hypothesized that the increase in diameter, accompanied by a reduction in bubble stability, resulted in a lower overall number density of microbubbles at the higher temperature. The results of the present study also indicate that the number of microbubbles contributing to the attenuation is reduced (by approximately 20%) for Definity at 37°C versus room temperature, as outlined in Table 3. Thus, our results obtained for Definity at body temperature are similar to the previously reported findings for the phospholipid-shelled contrast agent SonoVue. Conversely, the attenuation peak and the estimated number of microbubbles increased for MicroMarker and all three ELIP formulations.

Attenuation of MicroMarker (Fig. 4b) was not affected by an increase in temperature for frequencies from ~2 to 7 MHz, but was higher for frequencies >7 MHz. Peak attenuation for MicroMarker (6 MHz at 25°C) occurred at a slightly higher frequency (7 MHz) at 37°C. Both an increase in the shell stiffness parameter and a change in the relative size distribution of encapsulated microbubbles could be responsible for this frequency shift in peak attenuation. MicroMarker contains a high-molecular-weight gas with low solubility in aqueous solution, which promotes thermodynamic stability. Therefore, the change in frequency-dependent attenuation for frequencies >7 MHz is likely due to changes in the shell viscoelastic properties, which also depend on temperature. Although this agent was developed specifically for high-frequency imaging

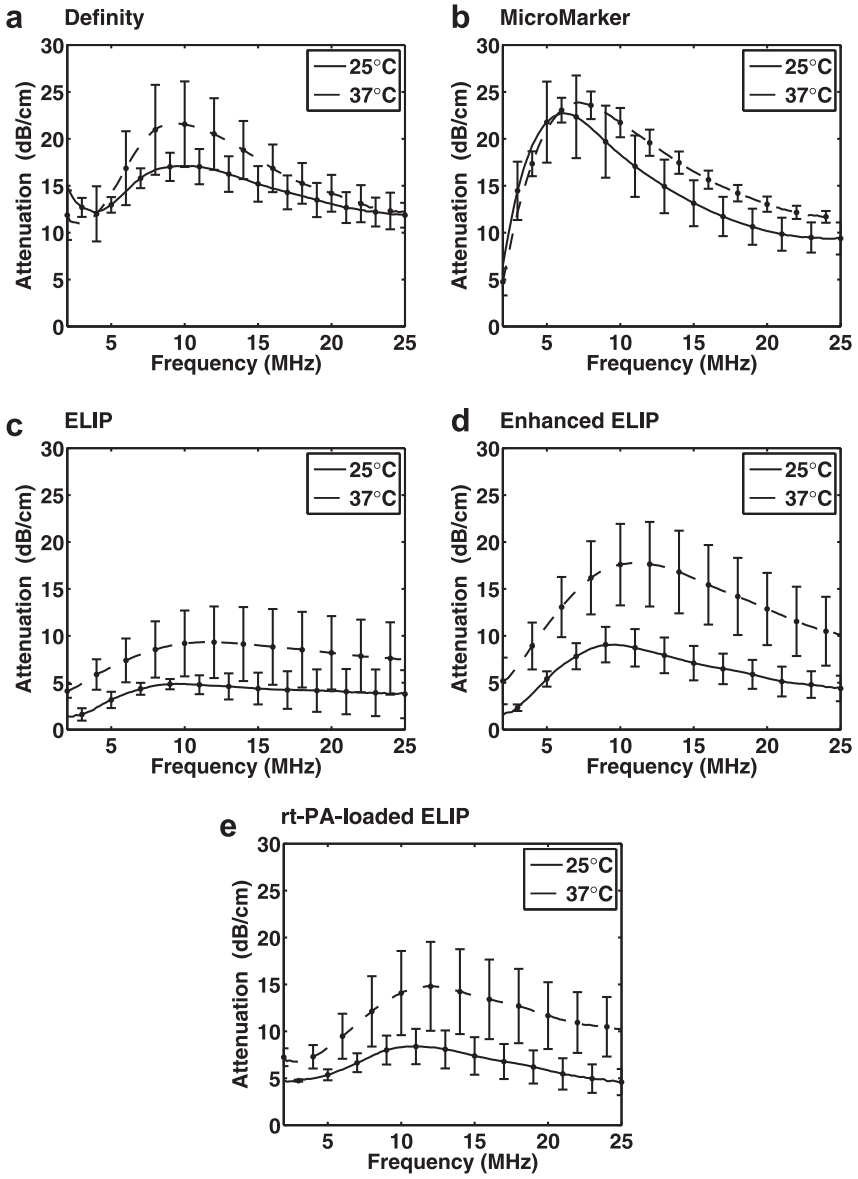


Fig. 4. Measured attenuation coefficients (±1 standard deviation) as a function of frequency at 25°C (*solid lines*) and 37°C (*dashed lines*) for (a) Definity, (b) MicroMarker, (c) echogenic liposomes (ELIP), (d) enhanced ELIP and (e) recombinant tissue plasminogen activator (rt-PA)-loaded ELIP.

applications, the frequency of peak attenuation for this agent was lower than for Definity and ELIP.

Echogenic liposomes exhibited higher attenuation at all frequencies at 37°C compared with room temperature (Figs. 4c–e). The increase in attenuation at 37°C occurs over a broad frequency range, which is consistent with an increase in the overall number of microbubbles and not simply a change in the relative size distribution. Our estimate of the number of microbubbles contributing to the attenuation ($N_{\text{fit}}$) supports this result (Table 3). However, the parameter $N_{\text{fit}}$ was determined from the attenuation data, and therefore, a causal relationship cannot be definitively established. It should be noted that a relatively small proportion of ELIP was found to contribute to the attenuation spectra, compared with Definity and MicroMarker, at either 25°C or 37°C. However, the number of particles that contribute to the attenuation (and, hence, are assumed to contain microbubbles) was two to three times higher at 37°C than at 25°C for each of the three ELIP formulations. The increase in the overall number of microbubbles could be due to the lower solubility of air in aqueous solution at 37°C relative to 25°C.

Sarkar et al. (2009) modeled the effects of encapsulation permeability, surface tension and diluent gas saturation on microbubble dissolution. In the model

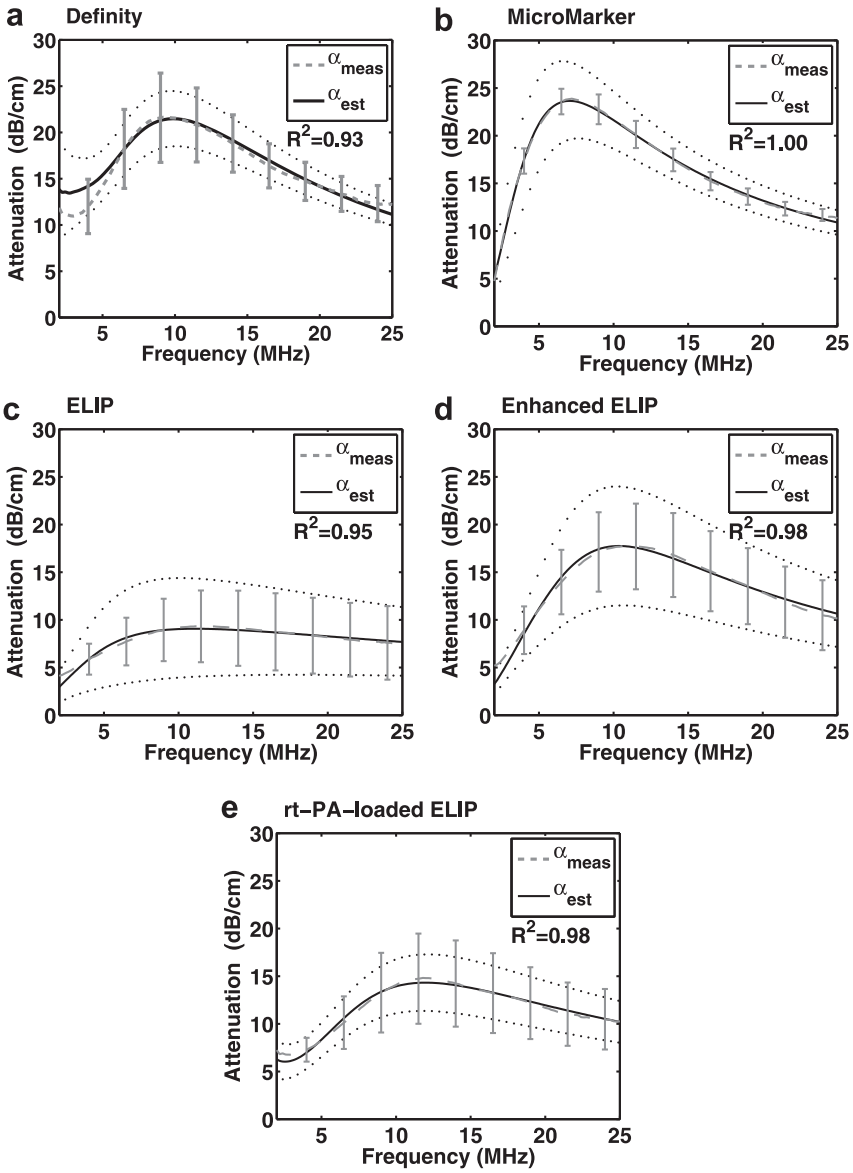


Fig. 5. Measured attenuation coefficients (±1 standard deviation) as a function of frequency (dashed lines) and theoretical fits (solid lines) based on the estimated shell parameters for (a) Definity, (b) MicroMarker, (c) echogenic liposomes (ELIP) and (d) enhanced ELIP and (e) recombinant tissue plasminogen activator (rt-PA)-loaded ELIP at 37°C. The dotted lines represent the confidence interval for the shell parameter fits given in Table 3.

presented, non-zero surface tension and under-saturation of the diluent are the primary forces that drive dissolution of UCAs (Sarkar et al. 2009). Under physiologic conditions, the solubility of air in the diluent is decreased, which would slow diffusion of gas through the lipid shell. Decreased permeability of the lipid shell at 37°C, which would mitigate gas exchange to some extent, may also account for the observed increased stability of ELIP under physiologic conditions (Buchanan et al. 2008).

Echogenic liposomes are thought to take on gas from the surrounding diluent (the stock solution) on reconstitution from the lyophilized state (Huang et al. 2002). Because the saturation partial pressure of gas in aqueous solution decreases at higher temperatures, it is possible that out-gassing from the fluid promotes diffusion of air into the liposomes and may also be responsible for the increase in attenuation at 37°C. This effect is similar to the observations of Kwan and Borden (2010). In their investigation of lipid-coated sulfur hexafluoride bubbles diluted in air-saturated fluid, the authors observed an influx of dissolved gas from solution, resulting in an initial expansion of the microbubbles. The expansion phase dynamics appeared to be dependent on the dynamic surface tension across the shell caused by the strong forces present between the lipid molecules. The authors hypothesized that higher defect densities

Table 3. Estimated number density of microbubbles and shell parameters for the UCAs*

| | | Number/mL | | | | |
|---|---|---|---|---|---|---|
| | $T$ | $N_{meas}/10^6$ | $N_{fit}/10^6$ | $S_p$ (N/m) | $S_f/10^{-6}$ (kg/s) | $R^2$ |
| Definity | 25°C | 4.82 ± 0.45 | 4.29 ± 0.89 | 1.76 ± 0.16 | 0.47 ± 0.05 | 0.93 |
| | 37°C | | 3.48 ± 1.26 | 1.10 ± 0.15 | 0.20 ± 0.04 | 0.93 |
| MicroMarker | 25°C | 5.31 ± 0.55 | 3.73 ± 0.45 | 1.20 ± 0.06 | 0.62 ± 0.03 | 1.00 |
| | 37°C | | 4.97 ± 0.41 | 1.90 ± 0.05 | 0.87 ± 0.02 | 1.00 |
| ELIP | 25°C | 1220 ± 320 | 2.07 ± 0.61 | 1.13 ± 0.13 | 0.82 ± 0.04 | 0.98 |
| | 37°C | | 6.10 ± 5.00 | 1.49 ± 0.20 | 1.41 ± 0.07 | 0.95 |
| Enhanced ELIP | 25°C | 590 ± 170 | 1.24 ± 0.12 | 1.98 ± 0.10 | 0.41 ± 0.03 | 1.00 |
| | 37°C | | 3.84 ± 1.06 | 3.10 ± 0.25 | 1.01 ± 0.07 | 0.98 |
| rt-PA-loaded ELIP | 25°C | 166 ± 40 | 2.05 ± 0.99 | 3.69 ± 0.76 | 1.88 ± 0.23 | 0.90 |
| | 37°C | | 4.06 ± 0.63 | 5.16 ± 0.37 | 2.09 ± 0.10 | 0.98 |

ELIP = echogenic liposomes; rt-PA = recombinant tissue plasminogen activator.
* The values of the shell parameters that corresponded to a doubling of the error function value were taken to be the limits for the confidence interval (Hoff 2001).

within the lipid shell may reduce the pressure buildup necessary for this expansion (Kwan and Borden 2010); importantly, defects in the lipid bilayer have been found to be important in promoting the echogenicity of ELIP (Huang et al. 2002).

The use of broadband PVDF transducers in the quantitative assessment of attenuation in this study resulted in a much larger usable bandwidth compared with our previous measurements (Kopechek et al. 2011). The frequency-dependent attenuation of ELIP (shown in Fig. 4c) agrees with our attenuation coefficients previously measured using a pulse-echo technique (Kopechek et al. 2011). Enhanced ELIP (shown in Fig. 4d) were more attenuative over all frequencies than ELIP. Furthermore, the enhanced ELIP formulation has a more rigid shell ($S_p$ = 3.10 ± 0.25, 37°C) than ELIP ($S_p$ = 1.49 ± 0.20, 37°C). The increased rigidity is consistent with Buchanan's hypothesis that a more rigid shell is responsible for reducing the loss of air and extending the duration of echogenic activity (Buchanan et al. 2008). ELIP loaded with the thrombolytic drug rt-PA exhibited greater attenuation than ELIP (Smith et al. 2010), but were approximately 3 dB less attenuative than the enhanced ELIP formulation.

*Limitations*

For the UCAs employed in this study, the use of low-amplitude (<100 kPa) broadband pulses was observed to result in a linear attenuation response. Therefore, the linearized theory proposed by de Jong et al. (1992; de Jong and Hoff 1993) was used to model the microbubbles in the linearly elastic regime. The amplitude of oscillations is assumed to be small and the microbubbles are assumed to respond in the linearly elastic regime. In addition, this model assumes that the acoustic scattering cross section is independent of the incident intensity and does not take multiple scattering effects into consideration. Higher-amplitude pulses, greater than approximately 100 kPa, led to non-linear oscillations that could be observed in the attenuation spectra. Our observation of the onset pressure threshold for non-linear effects in Definity was consistent with Chatterjee et al. (2005). However, the onset pressure depended on the agent as well as the temperature. Proper description of the microbubbles at these larger amplitudes would require the use of newer models that accurately capture the complex oscillatory dynamics of phospholipid-coated microbubbles, such as the model proposed by Marmottant et al. (2005).

The change in particle size distribution at 37°C versus 25°C was not assessed in this study because the Coulter counter measurements were conducted only at room temperature (25°C). It has recently been found that ELIP, when exposed to a decrease in temperature, lose their echogenicity (Kopechek et al. 2013; Radhakrishnan et al. 2012). The instrument used to measure the size distributions for this study was not equipped with a temperature control feature. To avoid exposure of ELIP and other UCAs to a reduction in temperature during the size measurement process and potential inaccurate sizing of the particles, the size distributions were measured only at room temperature.

## CONCLUSIONS

Frequency-dependent attenuation of several phospholipid-shelled UCAs was measured at 25°C and 37°C. The mean (volume-weighted) diameters of the UCAs measured were between 1.3 and 2.3 μm. Definity had a larger number of particles >5 μm in diameter than the other agents. As a diluent for the attenuation measurements, PBS with 0.5% (w/v) albumin was an adequate substitute for whole blood. Differences in shell parameters and estimated number density of the three types of UCAs were evident based on the attenuation

measurements over a broad frequency range, thus underscoring the importance of conducting characterization studies at physiologic temperature. Echogenic liposomes exhibited a larger increase in attenuation at 37°C versus 25°C than either Definity or MicroMarker. The enhanced ELIP formulation yielded a higher attenuation than the original formulation over the frequency band 2 to 25 MHz.

*Acknowledgments*—The authors thank Robert Giulitto (Hoxworth Blood Center) for assisting in the acquisition of human blood samples, Gail J. Pyne-Geithman (University of Cincinnati) for use of the blood gas analyzer and Jack Rubinstein (University of Cincinnati) for providing the MicroMarker contrast agent. The authors are also grateful to Melvin E. Klegerman (University of Texas Health Science Center at Houston) and members of the Image-Guided Ultrasound Therapeutics Laboratory (University of Cincinnati) for helpful discussions. This work was supported in part by the National Institutes of Health (NIH R01 HL74002, NIH R01 HL059586, NIH R01 NS047603, NIH F32 HL104916) and a grant-in-aid from the University of Cincinnati Chapter of Sigma Xi.

## REFERENCES

Alkan-Onyuksel H, Demos SM, Lanza GM, Vonesh MJ, Klegerman ME, Kane BJ, Kuszak J, Mcpherson DD. Development of inherently echogenic liposomes as an ultrasonic contrast agent. J Pharm Sci 1996;85:486–490.

Altman PL. Handbook of respiration. Philadelphia: Saunders; 1958.

AIUM Technical Standards Committee. Methods for specifying acoustic properties of tissue mimicking phantoms and objects; 1995, Laurel, MD: American Institute of Ultrasound in Medicine (AIUM).

Bekeredjian R, Grayburn PA, Shohet RV. Use of ultrasound contrast agents for gene or drug delivery in cardiovascular medicine. J Am Coll Cardiol 2005;45:329–335.

Buchanan KD, Huang S, Kim H, MacDonald RC, McPherson DD. Echogenic liposome compositions for increased retention of ultrasound reflectivity at physiologic temperature. J Pharm Sci 2008; 97:2242–2249.

Chatterjee D, Sarkar K, Jain P, Schreppler NE. On the suitability of broadband attenuation measurement for characterizing contrast microbubbles. Ultrasound Med Biol 2005;31:781–786.

Chen J, Zhu Z. Ultrasound attenuation in encapsulated microbubble suspensions: The multiple scattering effects. Ultrasound Med Biol 2006;32:961–969.

de Jong N, Hoff L. Ultrasound scattering properties of Albunex microspheres. Ultrasonics 1993;31:175–181.

de Jong N, Hoff L, Skotland T, Bom N. Absorption and scatter of encapsulated gas filled microspheres: Theoretical considerations and some measurements. Ultrasonics 1992;30:95–103.

Demos SM, Alkan-Onyuksel H, Kane BJ, Ramani K, Nagaraj A, Greene R, Klegerman M, McPherson DD. In vivo targeting of acoustically reflective liposomes for intravascular and transvascular ultrasonic enhancement. J Am Coll Cardiol 1999;33:867–875.

Elbayoumi TA, Torchilin VP. Liposomes for targeted delivery of antithrombotic drugs. Expert Opin Drug Deliv 2008;5:1185–1198.

Faez T, Goertz D, de Jong N. Characterization of Definity™ ultrasound contrast agent at frequency range of 5–15 MHz. Ultrasound Med Biol 2011;37:338–342.

Feinstein SB. Contrast ultrasound imaging of the carotid artery vasa vasorum and atherosclerotic plaque neovascularization. J Am Coll Cardiol 2006;48:236–243.

Goertz DE, de Jong N, van der Steen AF. Attenuation and size distribution measurements of Definity and manipulated Definity populations. Ultrasound Med Biol 2007;33:1376–1388.

Gorce JM, Arditi M, Schneider M. Influence of bubble size distribution on the echogenicity of ultrasound contrast agents: A study of SonoVue. Invest Radiol 2000;35:661–671.

Helfield BL, Huo X, Williams R, Goertz DE. The effect of preactivation vial temperature on the acoustic properties of Definity™. Ultrasound Med Biol 2012;38:1298–1305.

Hitchcock KE, Caudell DN, Sutton JT, Klegerman ME, Vela D, Pyne-Geithman GJ, Abruzzo T, Cyr PE, Geng YJ, McPherson DD, Holland CK. Ultrasound-enhanced delivery of targeted echogenic liposomes in a novel ex vivo mouse aorta model. J Control Release 2010;144:288–295.

Hoff L. Acoustic characterization of contrast agents for medical ultrasound imaging. Berlin/Heidelberg: Springer; 2001.

Hoff L, Sontum PC, Hovem JM. Oscillations of polymeric microbubbles: Effect of the encapsulating shell. J Acoust Soc Am 2000; 107:2272–2280.

Huang S. Ultrasound-responsive liposomes. In: Weissig V, (ed). Liposomes: Methods and protocols. New York: Humana Press; 2010.

Huang SL. Liposomes in ultrasonic drug and gene delivery. Adv Drug Deliv Rev 2008;60:1167–1176.

Huang SL, Hamilton AJ, Nagaraj A, Tiukinhoy SD, Klegerman ME, Mcpherson DD, Macdonald RC. Improving ultrasound reflectivity and stability of echogenic liposomal dispersions for use as targeted ultrasound contrast agents. J Pharm Sci 2001;90:1917–1926.

Huang SL, Hamilton AJ, Pozharski E, Nagaraj A, Klegerman ME, McPherson DD, MacDonald RC. Physical correlates of the ultrasonic reflectivity of lipid dispersions suitable as diagnostic contrast agents. Ultrasound Med Biol 2002;28:339–348.

Huang SL, MacDonald RC. Acoustically active liposomes for drug encapsulation and ultrasound-triggered release. Biochim Biophys Acta Biomembr 2004;1665:134–141.

Klegerman ME, Wassler M, Huang SL, Zou Y, Kim H, Shelat HS, Holland CK, Geng YJ, McPherson DD. Liposomal modular complexes for simultaneous targeted delivery of bioactive gases and therapeutics. J Control Release 2010;142:326–331.

Klibanov AL. Microbubble contrast agents: Targeted ultrasound imaging and ultrasound-assisted drug-delivery applications. Invest Radiol 2006;41:354–362.

Kopechek JA, Haworth KJ, Radhakrishnan K, Huang SL, Klegerman ME, McPherson DD, Holland CK. The impact of bubbles on measurement of drug release from echogenic liposomes. Ultrason Sonochem 2013;20:1121–1130.

Kopechek JA, Haworth KJ, Raymond JL, Douglas Mast T, Perrin SR Jr, Klegerman ME, Huang S, Porter TM, McPherson DD, Holland CK. Acoustic characterization of echogenic liposomes: Frequency-dependent attenuation and backscatter. J Acoust Soc Am 2011; 130:3472–3481.

Kornmann LM, Reesink KD, Reneman RS, Hoeks APG. Critical appraisal of targeted ultrasound contrast agents for molecular imaging in large arteries. Ultrasound Med Biol 2010;36:181–191.

Kwan JJ, Borden MA. Microbubble dissolution in a multigas environment. Langmuir 2010;26:6542–6548.

Laing ST, McPherson DD. Cardiovascular therapeutic uses of targeted ultrasound contrast agents. Cardiovasc Res 2009;83:626–635.

Lindner JR. Molecular imaging with contrast ultrasound and targeted microbubbles. J Nucl Cardiol 2004;11:215–221.

Marmottant P, van der Meer S, Emmer M, Versluis M, de Jong N, Hilgenfeldt S, Lohse D. A model for large amplitude oscillations of coated bubbles accounting for buckling and rupture. J Acoust Soc Am 2005;118:3499–3505.

Marsh JN, Hall CS, Hughes MS, Mobley J, Miller JG, Brandenburger GH. Broadband through-transmission signal loss measurements of Albunex® suspensions at concentrations approaching in vivo doses. J Acoust Soc Am 1997;101:1155–1161.

Mulvana H, Stride E, Hajnal JV, Eckersley RJ. Temperature dependent behavior of ultrasound contrast agents. Ultrasound Med Biol 2010; 36:925–934.

Patil H, Main ML. The history of product label changes for DEFINITY® in the US. US Cardiol 2012;9:35–39.

Paul S, Russakow D, Nahire R, Nandy T, Ambre AH, Katti K, Mallik S, Sarkar K. In vitro measurement of attenuation and nonlinear scattering from echogenic liposomes. Ultrasonics 2012;52:962–969.

Qin S, Caskey CF, Ferrara KW. Ultrasound contrast microbubbles in imaging and therapy: Physical principles and engineering. Phys Med Biol 2009;54:R27–R57.

Radhakrishnan K, Haworth KJ, Huang S-, Klegerman ME, McPherson DD, Holland CK. Stability of echogenic liposomes as a blood pool ultrasound contrast agent in a physiologic flow phantom. Ultrasound Med Biol 2012;38:1970–1981.

Sarkar K, Katiyar A, Jain P. Growth and dissolution of an encapsulated contrast microbubble: effects of encapsulation permeability. Ultrasound Med Biol 2009;35:1385–1396.

Sarkar K, Shi WT, Chatterjee D, Forsberg F. Characterization of ultrasound contrast microbubbles using in vitro experiments and viscous and viscoelastic interface models for encapsulation. J Acoust Soc Am 2005;118:539–550.

Smith DA, Vaidya SS, Kopechek JA, Huang SL, Klegerman ME, McPherson DD, Holland CK. Ultrasound-triggered release of recombinant tissue-type plasminogen activator from echogenic liposomes. Ultrasound Med Biol 2010;36:145–157.

Stapleton S, Goodman H, Zhou Y, Cherin E, Henkelman RM, Burns PN, Foster FS. Acoustic and kinetic behaviour of Definity in mice exposed to high frequency ultrasound. Ultrasound Med Biol 2009; 35:296–307.

Stride E. Physical principles of microbubbles for ultrasound imaging and therapy. Cerebrovasc Dis 2009;27(Suppl 2):1–13.

Stride E, Saffari N. Investigating the significance of multiple scattering in ultrasound contrast agent particle populations. IEEE Trans Ultrason Ferroelectr Freq Control 2005;52:2332–2345.

Sutton JT, Haworth KJ, Pyne-Geithman G, Holland CK. Ultrasound-mediated drug delivery for cardiovascular disease. Expert Opin Drug Deliv 2013;10:573–592.

Tiukinhoy-Laing SD, Huang S, Klegerman M, Holland CK, McPherson DD. Ultrasound-facilitated thrombolysis using tissue-plasminogen activator-loaded echogenic liposomes. Thromb Res 2007;119:777–784.

VisualSonics PN11691—Vevo MicroMarker™ Non-Targeted Contrast Agent Kit: Protocol and Information Booklet Rev 1.4. Toronto.

Vos HJ, Emmer M, de Jong N. Oscillation of single microbubbles at room versus body temperature. In: Proceedings, 2008 IEEE International Ultrasonics Symposium, Beijing, China, November 2–5, 2008. Beijing edition. New York: IEEE, 2008:982–984.

Weissig V. Liposomes: Methods and protocols. New York: Humana Press; 2010.

Whittle P. Prediction and regulation by linear least-square methods. 2nd rev. edition. Minneapolis, MN: University of Minnesota Press; 1983.